International Journal of Mechanical, Industrial and Aerospace Sciences
ISSN: 2517-9950
Vol:9, No:9, 2015

FEM Analysis of Occluded Ear Simulator with Narrow Slit Pathway

M. Sasajima, T. Yamaguchi, M. Watanabe, Y. Koike

***Abstract*—**This paper discusses the propagation of sound waves in air, specifically in narrow rectangular pathways of an occluded-ear simulator for acoustic measurements. In narrow pathways, both the speed of sound and the phase of the sound waves are affected by the damping of the air viscosity. Herein, we propose a new finite-element method (FEM) that considers the effects of the air viscosity. The method was developed as an extension of existing FEMs for porous, sound-absorbing materials. The results of a numerical calculation for a three-dimensional ear-simulator model using the proposed FEM were validated by comparing with theoretical lumped-parameter modeling analysis and standard values.

***Keywords*—**Ear simulator, FEM, simulation, viscosity.

I. Introduction

A conventional acoustic-analysis approach is used predominantly for relatively large structures and equipment. There are very few methods for analyzing the sound-propagation of equipment with a small volume, such as an occluded-ear simulator used for measurements of insert-type earphones, which was standardized by the international standard, IEC60318-4: Occluded-ear simulator for the measurement of earphones coupled to the ear by means of ear inserts (International Electro technical Commission, or IEC). Fig. 1 shows a space model of an inside-of-ear simulator. This ear simulator is often used for earphone and headphone measurements, and has very narrow pathways to control the acoustic resistance.

In narrow sound pathways, the speed and phase of the sound waves are affected by the damping of the air viscosity. Therefore, to conduct an accurate acoustic analysis of small equipment such as an ear simulator, the effect from the air viscosity should be considered, which is not typically done in a conventional acoustic analysis. In the present study, we propose a new finite-element method (FEM) that considers the effects of air viscosity in narrow areas of sound pathways. This method was developed as an extension of the acoustic FEMs proposed by Biot [1], [2] and Yamaguchi [3]–[5] for porous, sound-absorbing materials.

We attempted a numerical analysis in the frequency domain using our acoustic solver, which utilizes the proposed FEM [6].

M. Sasajima, M. Watanabe and Y. Koike are with the Strategic Development Division, Foster electric Co., Ltd., 196-8550, 1-1-109 Tsutsujigaoka, Akishima, Tokyo, (Phone: 042-847-3334; e-mail: sasajima@ foster.co.jp, Phone: 042-847-3334; e-mail: mtwatanabe@foster.co.jp, phone: 042-847-3334; e-mail: koike@ foster.co.jp).

T. Yamaguchi is with the School of Science and Technology, Gunma University, 376-8515, 1-5-1, Tenjin-cho, Kiryu, Gunma, Japan (e-mail: yamagme3@gunma-u.ac.jp).

For the numerical calculations, we used an occluded-ear simulator model having narrow rectangular cross sections. We compared the results obtained by the proposed FEM with those of a traditional lumped-parameter modeling (LPM) analysis and the international standard values of IEC60318-4.

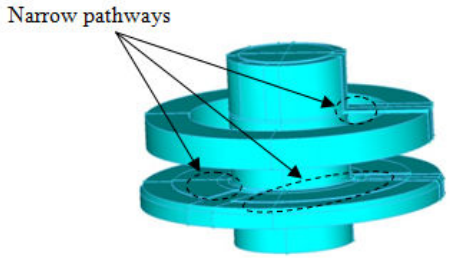

Fig. 1 Space model of inside-of-ear simulator

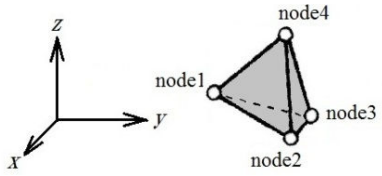

Fig. 2 Direct Cartesian coordinate system and constant strain element

II. Numerical Procedures

We developed a new FEM that incorporates the air viscosity at small amplitudes. Fig. 2 shows a direct Cartesian coordinate system, nodes, and a constant strain element of a three-dimensional (3D) tetrahedron. Here, u_x, u_y, and u_z are the displacements in the x, y, and z directions, respectively, at arbitrary points in the element. In this case, the strain energy $\tilde{U}$ is expressed as

$$\tilde{U} = \frac{1}{2} E \iiint_e \left(\frac{\partial u_x}{\partial x} + \frac{\partial u_y}{\partial y} + \frac{\partial u_z}{\partial z} \right)^2 dxdydz \quad , \tag{1}$$

where E is the bulk modulus of the air elasticity, and u is the time derivative of the particle displacement. Therefore, the kinetic energy $\tilde{T}$ is expressed as

$$\tilde{T} = \frac{1}{2} \iiint_e \rho \{u\}^T \{u\} dxdydz \quad , \tag{2}$$

where ρ is the effective density of the element, and T represents a transposition. The viscosity energy $\tilde{D}$ of a viscous fluid is expressed as

$$\tilde{D} = \iiint_e \frac{1}{2}\{\overline{T}\}^T \{\Gamma\} dxdydz \quad , \tag{3}$$

where $\{\overline{T}\}$ is the stress vector attributable to the viscosity. The relationship between the particle velocity and stress can be expressed as

$$\{\overline{T}\} \equiv \begin{Bmatrix} \tau_{xx} \\ \tau_{yy} \\ \tau_{zz} \\ \tau_{xy} \\ \tau_{yz} \\ \tau_{zx} \end{Bmatrix} = \begin{bmatrix} \frac{4}{3}\mu\frac{\partial}{\partial x} & -\frac{2}{3}\mu\frac{\partial}{\partial y} & -\frac{2}{3}\mu\frac{\partial}{\partial z} \\ -\frac{2}{3}\mu\frac{\partial}{\partial x} & \frac{4}{3}\mu\frac{\partial}{\partial y} & -\frac{2}{3}\mu\frac{\partial}{\partial z} \\ -\frac{2}{3}\mu\frac{\partial}{\partial x} & -\frac{2}{3}\mu\frac{\partial}{\partial y} & \frac{4}{3}\mu\frac{\partial}{\partial z} \\ \mu\frac{\partial}{\partial y} & \mu\frac{\partial}{\partial x} & 0 \\ 0 & \mu\frac{\partial}{\partial z} & \mu\frac{\partial}{\partial y} \\ \mu\frac{\partial}{\partial z} & 0 & \mu\frac{\partial}{\partial x} \end{bmatrix} \begin{Bmatrix} \dot{u}_x \\ \dot{u}_y \\ \dot{u}_z \end{Bmatrix}, \tag{4}$$

where u_x, u_y, and u_z are the particle velocities in the x, y, and z directions at arbitrary points in the element, respectively, and μ is the coefficient of viscosity of the medium. In the above equation, $\{\Gamma\}$ is the strain vector. Next, we considered the formulation of a motion equation of an element for an acoustic-analysis model used to consider the viscous damping. The potential energy $\tilde{V}$ is expressed as

$$\tilde{V} = \int_\Gamma \{u\}^T \{\overline{P}\} d\Gamma + \iiint_e \{u\}^T \{F\} dxdydz \quad , \tag{5}$$

where $\{\overline{P}\}$ is the surface force vector, $\{F\}$ is the body force vector, and $\int_\Gamma d\Gamma$ is the integral of the element boundary. The total energy $\tilde{E}$ is derived using

$$\tilde{E} = \tilde{U} + \tilde{D} - \tilde{T} - \tilde{V}. \tag{6}$$

Using Lagrange's equations, we obtain the following discretized equation for an element:

$$\frac{d}{dt}\frac{\partial \tilde{T}}{\partial \dot{u}_{ei}} - \frac{\partial \tilde{T}}{\partial u_{ei}} + \frac{\partial \tilde{U}}{\partial u_{ei}} - \frac{\partial \tilde{V}}{\partial u_{ei}} + \frac{\partial \tilde{D}}{\partial u_{ei}} = 0 \quad , \tag{7}$$

where u_{ei} is the i^{th} component of the nodal displacement vector $\{u_e\}$, and $\dot{u}_{ei}$ is the i^{th} component of the nodal particle-velocity vector $\{\dot{u}_e\}$. We obtain the following discretized equation of an element by substituting (1)–(5) into (7):

$$-\omega^2[M_e]\{u_e\} + [K_e]\{u_e\} + j\omega[C_e]\{u_e\} = \{f_e\}. \tag{8}$$

Here, we use $\{\dot{u}_e\} = j\omega\{u_e\}$ because a periodic motion with angular frequency ω is assumed. In addition, $[M_e]$, $[K_e]$, $[C_e]$, and $\{f_e\}$ are the element-mass matrix, element-stiffness matrix, element-viscosity matrix, and nodal force vector, respectively. All nodal particle displacements can be calculated by solving (8). In addition, the strain and sound pressure of all elements can be calculated from the nodal particle displacements.

III. Calculation

A. Damping Analysis using Proposed 3D FEM

To verify our method, we conducted an acoustic-damping analysis of inside the ear simulator. As shown in Fig. 3, the model used is a half-solid and is symmetrical about the center plane, with a height of 14.0 mm, and a main cavity radius of 7.5 mm. Narrow pathways from the main cavity lead to two Helmholtz resonance cavities at heights of only 0.69 and 0.17 mm. The size of the two resonators of ring shape is as the size occurring resonance at 1,800 Hz and 5,000 Hz. The model employs tetrahedral elements with four nodes, and we used HyperMesh v12.0 (Altair Engineering Inc.) for the meshing. The narrow pathways were divided into five elements in the height direction.

The boundary conditions are similar between both ends of the main cavity. We set the effective density as $\rho_0 = 1.2$ kg/m^3, the coefficient of viscosity μ as 1.82×10^{-5} Ns/m^2, the real part of the complex volume elasticity E_0 as 1.4×10^5 Pa, and the sound propagation speed c as 340 m/s in air. The excitation surface was on top of the main cavity. The reference point was the center of the bottom of the main cavity. For the boundary conditions, the particle displacements of all nodes on the outside in contact with the surfaces were fixed, with exception of the nodes in the plane of symmetry.

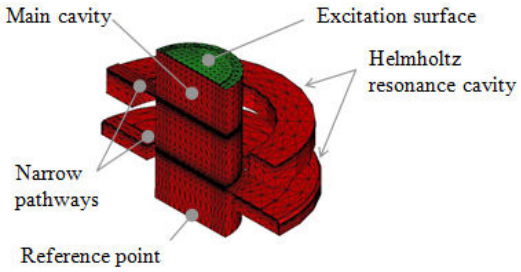

Fig. 3 3D model for FEM (1/2 symmetric model)

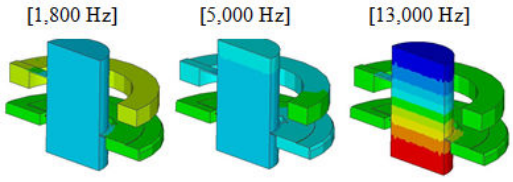

Fig. 4 Distribution of element pressure at each resonance

Fig. 4 shows contours for the calculated element pressure of the model for the proposed FEM near the resonance conditions of the two annular Helmholtz resonance cavities and the main

cylindrical cavity. Red indicates a high presser, whereas blue indicates a low presser. Fig. 5 shows contours for the calculated particle displacements, and is a surface view of the model. Here, red indicates a large amount of displacement, and blue indicates a small amount of displacement. The isosurface of the displacement of the particles changes significantly in the narrow pathway at 1,800 Hz.

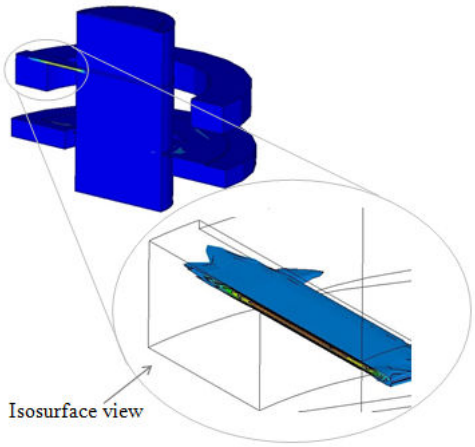

Fig. 5 Distribution of particle-displacement contour in a surface view of the narrow pathway (1,800 Hz)

Fig. 6 shows the analysis results of the bottom reference point for the sound-pressure level versus the frequency obtained using the aforementioned model. Here, the sound-pressure level is normalized at 500 Hz.

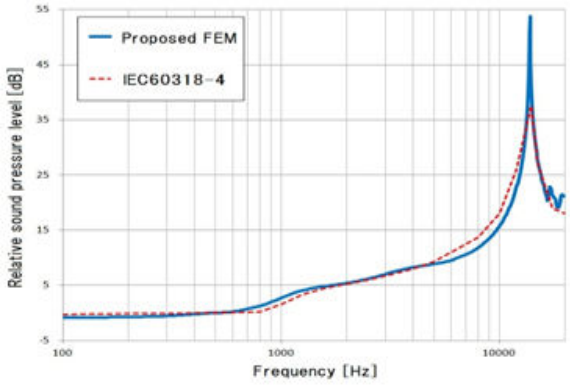

Fig. 6 Normalized sound-pressure level of proposed FEM

B. Theoretical Damping Analysis

To verify the results of the proposed FEM, we conducted a theoretical analysis using LPM for the frequency domain, which is widely used for simulations of acoustic equipments simulation. The equivalent electrical circuit diagram of the LPM model for the ear simulator is shown in Fig. 7 [7]. The electrical resistance (Ra), inductance (ma), and capacitance (Ca) match the acoustical resistance, mass, and compliance, respectively.

In this LPM model, the resistances of the narrow pathways are Ra5 and Ra7, which represent the effect of the air viscosity. Therefore, the ear simulator is tuned by adjusting the height of the narrow pathways to control the middle frequency property. The masses of air in the narrow pathways are ma5 and ma7, and the compliances of the Helmholtz resonators are Ca5 and Ca7.

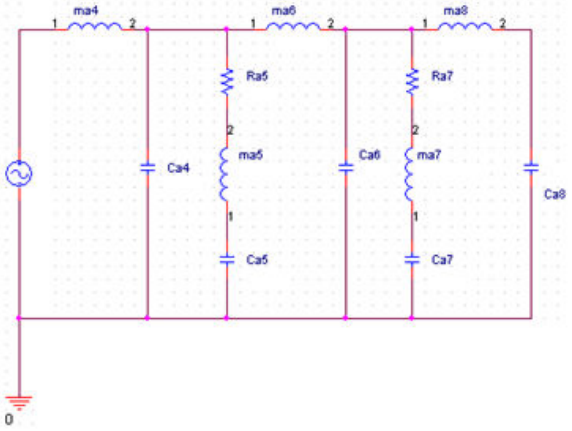

Fig. 7 Impedance-type equivalent circuit diagram of the ear simulator

We employed the following parameters from the IEC60318-4 standard, which are based on acoustical-impedance measurements of the average impedance of the human ear.

$r_{a5} = 506\ \Omega$

$r_{a7} = 311\ \Omega$

$_{ma4} = 78.8 \times 10^{-5}$ H, $C_{a4} = 0.09\ \mu$F

$_{ma5} = 9.4 \times 10^{-2}$ H, $C_{a5} = 0.19\ \mu$F

$_{ma6} = 132.3 \times 10^{-5}$ H, $C_{a6} = 0.153$ F

$_{ma7} = 983.8 \times 10^{-5}$ H, $C_{a7} = 0.218$ F

$_{ma8} = 153.5 \times 10^{-5}$ H, $C_{a8} = 0.215$ F

Fig. 8 shows the analysis results for the transfer impedance with respect to the frequency obtained using the LPM model [8], [9]. The highest frequency peak at about 12,800 Hz is due to the resonance of the main cavity. The two Helmholtz resonators resonate, and the two narrow pathways control the characteristics within the middle frequency region.

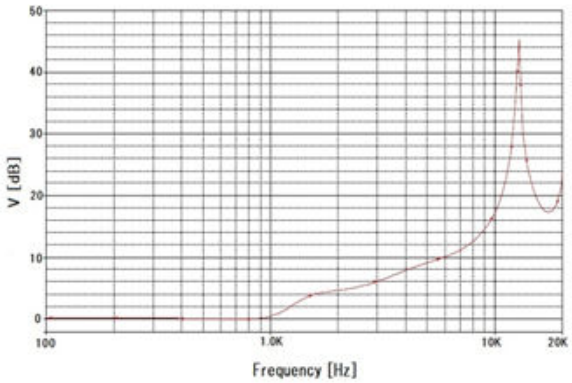

Fig. 8 Impedance of LPM simulation model (IEC60318-4 standard)

C. Verification and Comparison of Proposed Method

We analyzed the frequency responses using the proposed FEM, and then compared the results of the numerical calculation with the IEC60318-4 standard values of the LPM simulation model property. Fig. 9 shows the analysis results for the pressure with respect to the frequency response obtained using the proposed FEM, along with the IEC60318-4 standard values, and standard upper and lower tolerances.

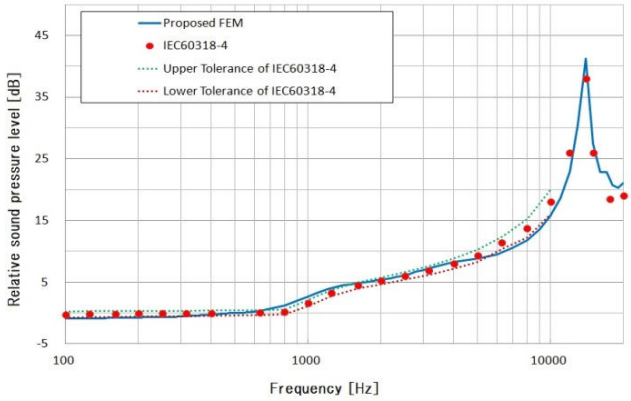

Fig. 9 Pressure with respect to the frequency response for the tube model

As shown in Fig. 9, the results of the proposed FEM are almost within the range of tolerance throughout the frequency domain. The results are particularly accurate for the frequency band defined in the standard. However, the tolerance range of the standard is defined only for frequency ranges of 100 to 10,000 Hz. Thus, the proposed FEM accurately represents the effect of the suppression of two Helmholtz resonance peaks (1,800 and 5,000 Hz) from the air viscosity.

IV. Conclusion

In this paper, we proposed a new acoustic FEM that considers the effects of air viscosity at in narrow acoustic pathways. We conducted a 3D finite-element analysis of an occluded-ear simulator for acoustic equipment with narrow sound pathways. Comparing the results obtained with those of an analysis using the LPM model defined by IEC60318-4 and the standard value shows that the proposed acoustic FEM exhibits good analytical accuracy. Frequency property that includes the effects of attenuation and Helmholtz resonance in the middle range can consider to accurately simulating throughout frequency range.

For future development, we plan to use this model for an accurate acoustic simulation of our high-quality earphones and headphones. Using this analysis technique in the design process of such devices, the frequency property of the product can be rapidly predicted.

This will help in reducing the number of trial prototypes and the development period. In addition, we aim to improve the speed of development and the technical skills of the engineers based on a greater understanding of the mechanism inherent to particular phenomena through detailed acoustic simulations.

References

[1] M. A. Biot, "Theory of propagation of elastic waves in a fluid-saturated porous solid. I. Low-frequency range," *Journal of Acoustical Society of America*, vol. 28, pp. 168–178, 1956.

[2] M. A. Biot, "Theory of propagation of elastic waves in a fluid-saturated porous solid. II. Higher-frequency range," *Journal of Acoustical Society of America*, vol. 28, pp. 179–191, 1956.

[3] T. Yamaguchi, H. Nakamoto, Y. Kurosawa, and S. Matsumura "Finite element analysis for damping properties of sound-proof structures having solid body, porous media and air," *Transactions of the Japan Society of Mechanical Engineers, Series C*, vol. 69, no. 677, pp. 34–41, 2003.

[4] Y. Kurosawa and S. Matsumura "Finite element analysis for damping properties of sound-proof structures having solid body, porous media and air," *Transactions of the Japan Society of Mechanical Engineers, Series C*, vol. 69, no. 677, pp. 34–41, 2003.

[5] T. Yamaguchi, J. Tsugawa, H. Enomoto, and Y. Kurosawa, "Layout of Sound Absorbing Materials in 3D Rooms Using Damping Contributions with Eigenvectors as Weight Coefficients," *Journal of System Design and Dynamics*, vol. 4-1, pp. 166–176, 2010.

[6] T. Yamaguchi, Y. Kurosawa, and H. Enomoto, "Damped Vibration Analysis Using Finite Element Method with Approximated Modal Damping for Automotive Double Walls with a Porous Material," *Journal of Sound and Vibration*, vol. 325, pp. 436–450, 2009.

[7] M. Sasajima, T. Yamaguchi, and A. Hara, "Acoustic Analysis Using Finite Element Method Considering Effects of Damping Caused by Air Viscosity in Audio Equipment," *Applied Mechanics and Materials*, vol. 36, pp. 282–286, 2010.

[8] IEC60318-4, IEC standard, Simulators of human head and ear - Part 4: Occluded-ear simulator for the measurement of earphones coupled to the ear by means of ear inserts 2010.

[9] S. Jonsson, B. Liu, A. Schuhmacher and L. Nielsen, "Simulation of the IEC 60711 occluded ear simulator," *Audio Engineering Society 116th convention*, 2004.